Ind. J. Pharm. Edu. Res., 2026; 60(3):1206-1217.
https://www.ijper.org

Original Article

Decoding the Anticancer Mechanism of Action of Kaempferol in Liver Cancer Cells via Transcriptomics, Network Pharmacology, Molecular Docking, Dynamics Simulations, and *in vitro* Validation

Zhen He[1,#], Wei Liu [2,#], Na Su[3], Guoqiang Xing[4,*]

[1]Department of Oncology, Wuhan Third Hospital, Tongren Hospital of Wuhan University, Wuhan Hubei, CHINA.
[2]Department of Liver Disease, Yantai Qishan Hospital, Yantai, Shandong, CHINA.
[3]Department of Critical Care Medicine, Shaanxi Rehabilitation Hospital, Xi'an Shaanxi, CHINA.
[4]Department of Oncology, The First Hospital of Weinan, Weinan Shaanxi, CHINA.
[#]Zhen He and Wei Liu are co-first authors, they contributed equally to this work.

ABSTRACT

Background: Kaempferol, a dietary flavonoid with proven antioxidant and antiinflammatory properties, has garnered significant interest in cancer research for its ability to modulate multiple oncogenic pathways, making it a compelling candidate for multitargeted therapy in addressing the considerable health burden of liver cancer. **Objectives:** To elucidate the therapeutic potential of kaempferol through network pharmacology, and *in vitro* experimental methodology. **Materials and Methods:** The pharmacological and physico-chemical properties of kaempferol were assessed using SwissADME and Protox-3.0. Target prediction utilized SuperPred and SwissTargetPrediction, filtered for liver cancer-specific genes through GeneCards. Protein-Protein Interaction (PPI) networks were constructed in Cytoscape, with hub genes identified via cytoHubba. Functional enrichment analyses, molecular docking, and dynamics were conducted, supported by GEPIA2 and TIMER analyses. HEP-G2 cell assays evaluated cell cytotoxicity, cell migration, apoptosis, and cell cycle phase distribution effects. **Results:** Kaempferol exhibited favorable drug-likeness, low toxicity, and potent interactions with liver cancer targets. Hub genes (GSK3B, MMP9, STAT1) were identified, linked to key cancer pathways (Wnt, PI3K-Akt, ECM-receptor). Molecular docking demonstrated high affinity for GSK3B (-8.9 kcal/mol), MMP9 (-9.2 kcal/mol), and STAT1 (-7 kcal/mol), with stable interactions validated by dynamics. Expression analyses revealed upregulation of these genes in liver cancer, correlated with immune infiltration patterns. Experimentally, kaempferol reduced HEP-G2 cell viability in a dose-dependent manner, significantly inhibited cell migration, induced cell apoptosis (early and late), and arrested cells at the G2/M phase. **Conclusion:** Kaempferol regulates critical pathways in liver cancer, exhibiting potent anticancer effects through induction of apoptosis, inhibition of cell migration, and cell cycle arrest, thereby positioning it as a compelling prospect for therapeutic development.

Keywords: Natural Products, Bioinformatics, Network Pharmacology, Liver cancer, Molecular Docking, Apoptosis.

Correspondence:
Dr Guoqiang Xing
Department of Oncology, The First Hospital of Weinan, Weinan Shaanxi-714000, CHINA.
Email: xingguoqiang55@hotmail.com
ORCID: 0009-0004-8920-169X

Received: 14-12-2025;
Revised: 09-02-2026;
Accepted: 27-03-2026.

INTRODUCTION

Hepatocellular Carcinoma (HCC), the most prevalent kind of primary liver cancer, constitutes 75% of all instances.[1] It is the 6th most frequent malignancy globally and the 4th largest cause of cancer-related deaths worldwide.[2] Notwithstanding advancements in early detection techniques and therapeutic alternatives for HCC, some patients continue to encounter a poor prognosis, mostly attributable to the aggressive disease characteristics and late diagnosis.[1,2] Standard treatments now available, including surgical excision, liver transplantation, and localised interventions such as radiofrequency-ablation and transarterial-chemoembolization, demonstrate optimal efficacy in individuals with early-stage or localised tumours.[3,4] Established therapeutic modalities, including surgical excision, organ transplantation, and localised therapies, exhibit optimum effectiveness in handling patients with early-stage or localised malignancies.[5,6] A significant obstacle in current therapeutic approaches is the development of treatment resistance, often

DOI: 10.5530/ijper.20262120

induced by biological mechanisms such as cancer cell plasticity and epithelial-mesenchymal transition. These pathways not only promote the dissemination of cancer cells but also augment their capacity to circumvent therapeutic measures, leading to worse patient outcomes and treatment resistance.

The polyphenolic compounds found in plants, known as flavonoids, make up a significant amount of the human diet.[7] Among these compounds, the flavonoid kaempferol stands out as having great potential as a cancer fighter.[8] Many foods, including apples, beans, broccoli, tea, and strawberries, are high in kaempferol.[9] Studies have shown that it activates many pathways that have a role in the control of cancer cells. Even though it strongly promotes cancer cell apoptosis, kaempferol also modulates other cell signalling cascades.[10] Kaempferol is also gentler on normal cells than traditional chemotherapy drugs making it a viable candidate cancer therapy. Kaempferol has garnered significant interest in cancer research for its ability to modulate multiple oncogenic pathways, making it a compelling candidate for multitargeted therapy in addressing the considerable health burden of liver cancer.

Network pharmacology, *in silico* molecular docking and dynamics, and bioinformatics collectively streamline the discovery and development of natural-product-derived therapeutics, Traditional Chinese Medicine (TCM) and other herbal formulations by integrating systems-level insight with atomistic characterization.[11,12] Network pharmacology results in the construction of compound-target-pathway networks to reveal multi-targeted actions and synergistic relationships among herbal constituents, enabling a holistic understanding of efficacy and safety profiles.[13] *In silico* docking rapidly screens bioactive compounds against potential protein targets to predict binding affinities and modes, while molecular dynamics simulations refine these complexes over time, assessing stability and conformational flexibility under physiologically relevant conditions.[14] Complementary bioinformatics analyses such as gene expression profiling, pathway enrichment, and immune-infiltration correlation, validate computational predictions within biological contexts and identify biomarkers of response.[11,12] By integrating these computational approaches, researchers can prioritize high-value natural compounds, reduce dependency on trial-and-error experimentation, and accelerate the translation of TCM knowledge into evidence-based, multi-target drug candidates.

This study aims to investigate the potential of kaempferol in targeting liver cancer, leveraging its capacity to analyse extensive biological datasets and discern molecular mechanisms. Utilising bioinformatics tools, we estimated interactions of kaempferol with essential pathways, particularly those associated with liver cancer progression and resistance. The insights guided the experimental design, enabling a targeted approach towards specific biomarkers and pathways. The use of experimental models, such as cell-based assays, effectively validated bioinformatics predictions, thereby confirming the anticancer activity of kaempferol. This comprehensive approach improves our understanding of the therapeutic potential of kaempferol and highlights the significance of bioinformatics in the progression of cancer research (Figure 1). However, its scope is confined to single hepatocellular carcinoma cell line, limiting generalizability across diverse genetic backgrounds and tumor microenvironments. The absence of *in vivo* or clinical data precludes assessment of pharmacokinetics, systemic toxicity, and therapeutic efficacy in whole organisms, and the reliance on predicted targets necessitates further biochemical validation to confirm mechanism specificity and offtarget interactions.

MATERIALS AND METHODS

Physicochemical characteristics of kaempferol

The druglikeness of kaempferol, which involved solubility, molecular weight, lipophilicity, and pharmacokinetic/pharmacodynamic parameters, were determined through SwissADME tool ("https://www.swissadme.ch/").[15] The ADME profile as well as the drug-likeness along with medicinal chemistry properties of a molecule are assessed from this source. The Protox-3.0 server was then applied to calculate further toxicological profiling by prediction levels of kaempferol including cytotoxic, hepatotoxic and carcinogenic ("https://tox.charite.de/protox3/").[16]

Target predictions for kaempferol

The possible molecular targets of kaempferol were predicted utilising a chemical similarity technique and a comprehensive database of compound-protein interactions via the use of SuperPred, an online platform ("https://prediction.charite.de/subpages/target_prediction.php").[17] Additionally, SwissTargetPrediction ("http://www.swisstargetprediction.ch/") was used to ascertain prospective biological targets based on the 2D and 3D structural attributes of kaempferol, therefore offering a comprehensive investigation of its interaction capacity.[18] By integrating these complementary platforms-machine-learning-driven, ATC-aware framework of SuperPred and dual-similarity, species-specific approach of SwissTargetPrediction-researchers can achieve broad, accurate, and rapid *in silico* identification molecular targets, providing a strong foundation for subsequent experimental validation. Both the results files were filtered with probability filter of ≥65% and then combined to eliminate duplicate entries.

Target prediction liver cancer

GeneCards was used to get liver cancer-specific targets by querying the keyword "Liver Cancer" ("https://www.genecards.org/").[19] It amalgamates genomic, proteomic, and transcriptome analyses to provide extensive information about genes implicated

in the genesis and progression of liver cancer. The target screening was performed by setting the GIFTS score at ≥55.

Kaempferol and liver cancer common targets and network construction

Using JVenn, an online tool for generating Venn diagrams and analyzing overlapping gene sets, common targets between kaempferol and liver cancer were identified ("https://jvenn.toulouse.inrae.fr/app/index.html").[20] For the construction of PPI networks, a comprehensive map of molecular interactions based on experimental as well as computational evidence is made available by the STRING database ("https://string-db.org/").[21] Cytoscape, a software package that has been designed for the investigation and picturing of complex networks, was used to investigate the resulting PPI network. Using the cytoHubba plug-in inside Cytoscape, the hub genes critical nodes in the PPI network of interest were found based on topological parameters.

Gene-Ontology and KEGG pathway assessments

The kaempferol hub targets were functionally annotated and pathway enrichment analyses were conducted using the ShinyGo database ("https://bioinformatics.sdstate.edu/go/").[22] This platform would provide insight into the Biological Processes (BP), Molecular Functions (MF), and Cellular Components (CC) associated with the identified targets, particularly KEGG pathways relevant to liver cancer in our case.

Expression Analysis using GEPIA

Using GEPIA2, "Gene Expression Profiling Interactive Analysis 2", we compared the expression levels of kaempferol targeted hub genes in normal tissues with those in liver cancer.[23] Differential expression, survival, and correlation investigations of hub genes are made possible by this online service that incorporates RNA sequencing data from the TCGA and GTEx projects. Available at: https://gepia2.cancer-pku.cn/#index

Effects on Tumor Microenvironment (TME)

TME studies of kaempferol impact were evaluated through the TIMER (Tumor Immune Estimation Resource) server.[24] TIMER server provides in-depth immune infiltration analysis and explores the correlation between different immune cell populations and hub gene expression. TIMER leverages TCGA data to estimate the abundance of immune cell infiltrates-such as T cells, B cells, macrophages, neutrophils, and dendritic cells-in tumor tissues across diverse cancer types, enabling researchers to correlate specific gene expression with immune infiltration patterns (e.g., high $CD8^+$ T cell levels), compare gene expression between tumor and normal tissues, and generate Kaplan-Meier survival plots that integrate gene expression and immune contexture for identifying prognostic biomarkers and immunerelated therapeutic targets. Available at: http://timer.cistrome.org/

Molecular docking and Dynamics

Kaempferol was prepared using ChemDraw to optimize the chemical structure and assign charges. Protein structures for GSK3B, MMP9, and STAT1 (1h87, 1gkc and 8d3f) were obtained from the RCSB PDB and prepared in BIOVIA Discovery Studio where water molecules were removed, hydrogens added, and charges assigned. These prepared structures were then uploaded to CB-Dock2 (online molecular docking server available at: "https://cadd.labshare.cn/cb-dock2/index.php") that predicted curpockets or potential active sites on the proteins.[25] It performs blind docking. Kaempferol was free to bind at any point of the protein's surface. Interactions were viewed using Discovery Studio, which allows for 2D and 3D images of ligand-protein interaction, including highlighting key binding residues and interactions.

Chemicals and Reagents

Kaempferol (Sigma-Aldrich, St. Louis, MO, USA; Cat. No. K0133); Dulbecco's Modified Eagle Medium (DMEM; Gibco, Grand Island, NY, USA; Cat. No. 11965-092); Fetal Bovine Serum (FBS; Gibco; Cat. No. 16000-044); Penicillin-Streptomycin (Gibco; Cat. No. 15140-122); MTT reagent (Sigma-Aldrich; Cat. No. M5655); FITC Annexin V Apoptosis Detection Kit I (BD Biosciences, San Jose, CA, USA; Cat. No. 556547); Propidium Iodide (Sigma-Aldrich; Cat. No. P4170); and Ribonuclease A (Sigma-Aldrich; Cat. No. R6513).

Cell Culture

The THLE-2 (normal liver cell line; Cat. no. #CRL-2706; ATCC, Manassas, USA) and HEP-G2 (liver cancer cell line; Cat. no. HB-8065; ATCC, Manassas, USA). Cells were cultured in DMEM (Gibco, NY, USA) supplemented with 10% FBS (Gibco, Grand Island, NY, USA) and 1% penicillin-streptomycin under standard conditions (37°C, 5% CO_2). Cells were subcultured every 2-3 days and seeded into appropriate culture plates (depending on assay type) at a density of $1x10^5$ cells per well for treatment with kaempferol. The cell lines were grown to 80% confluency before being exposed to varying concentrations of kaempferol (0, 15, 30, 60, and 120 µM). DMSO served as a vehicle control, and cells were incubated for 24 or 48 hr depending on the assay. All experiments were performed in triplicates to ensure reproducibility.

Viability Assessment

To evaluate the cytotoxic effects of kaempferol on HEP-G2 cells, the cells were treated with increasing concentrations (0, 15, 30, 60, and 120 µM) of kaempferol for 24 hr. Cell viability was assessed using the MTT assay, where MTT reagent was added to each well and incubated for 4 hr at 37°C. The resulting formazan crystals were dissolved in DMSO, and the absorbance was measured at 570 nm using a microplate reader (BioTek Instruments, VT, USA). Cell viability was expressed as a percentage of control cells (0 µM kaempferol), with each experiment conducted in triplicate.

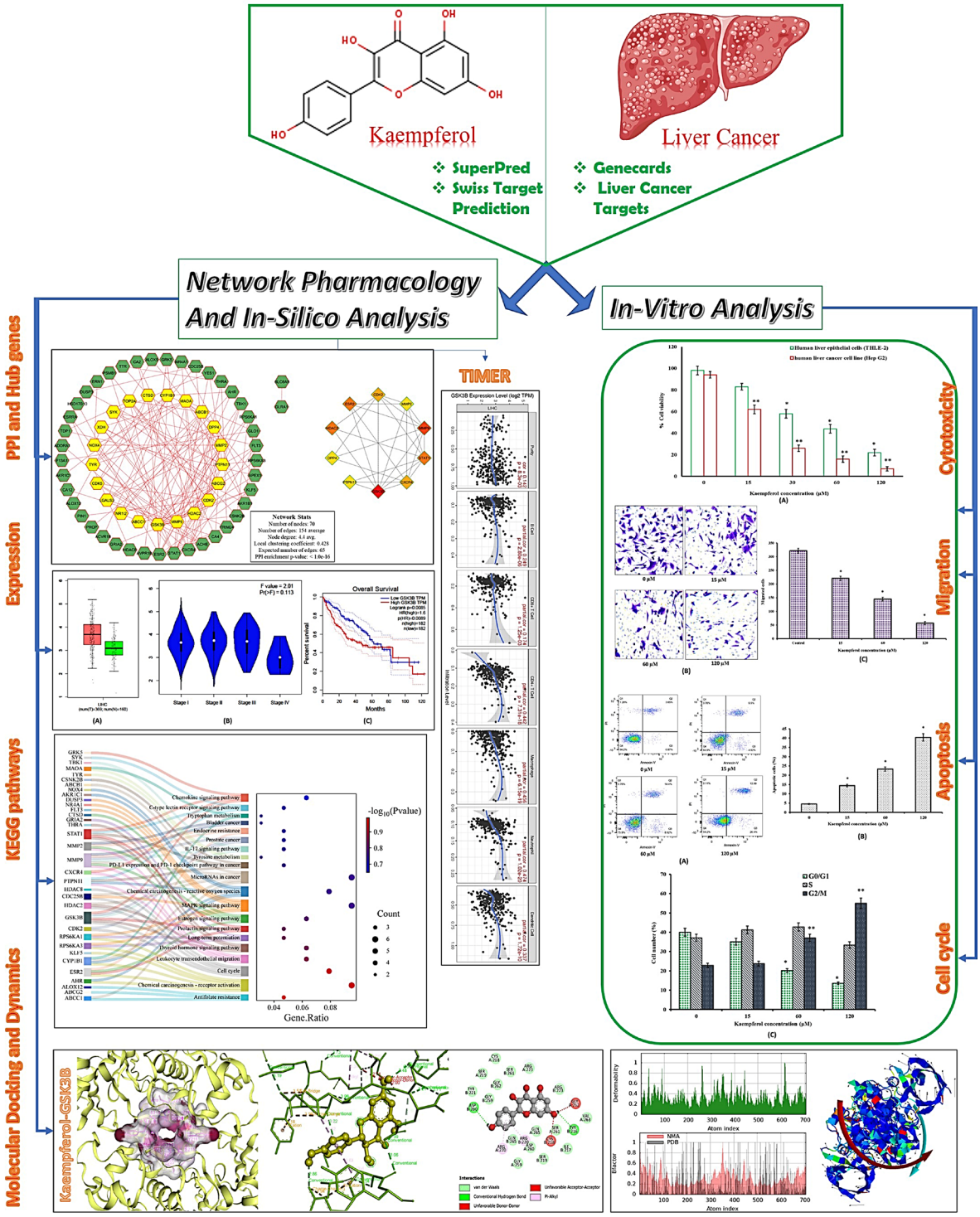

Figure 1: Flow chart illustrating the study design and methodology adopted for the current research work.

Transwell Assay for Migration

The migration ability of HEP-G2 cells treated with kaempferol was assessed using a Transwell migration assay. Cells were serum-starved for 24 hr before being resuspended in serum-free media and seeded into the upper chambers of a Transwell insert (8.0 µm pore size membrane; Corning, NY, USA; Cat. No. #3428). The lower chamber contained DMEM with 10% FBS as a chemoattractant. Cells were treated with kaempferol concentrations of 0, 15, 60, and 120 µM for 24 hr. Following incubation, the migratory cells were identified by fixing them with methanol, staining them with crystal violet, and counting them under a light microscope. The surface of the membrane was cleaned of cells that had not migrated. Cell migration was quantified by counting cells in five randomly chosen fields per well, and each treatment was examined in triplicate.

Annexin V/PI Staining

To analyze apoptosis induced by kaempferol in HEP-G2 cells, Annexin V-FITC and Propidium Iodide (PI) staining was performed by a FITC Annexin V Apoptosis Detection Kit (BD Biosciences, USA). Cells were treated with 0, 15, 60, and 120 µM kaempferol for 24 hr, then harvested and washed with PBS. The cells were resuspended in binding buffer, and Annexin V-FITC was added to label early apoptotic cells, followed by PI staining to identify late apoptotic or necrotic cells. After incubation for 15 min at room temperature in the dark, samples were analyzed by Attune™ NxT Flow Cytometer (Thermo Fisher Scientific Inc., Waltham, MA, USA). The apoptotic population was quantified by measuring the fluorescence intensities of Annexin V and PI, with each condition tested in triplicate.

Cell Cycle (Flow Cytometry)

Cell cycle analysis was performed to assess the effect of kaempferol on the progression of HEP-G2 cells. After treatment with 0, 15, 60, and 120 µM kaempferol for 24 hr, cells were harvested and fixed in 70% ethanol overnight at 4°C. The fixed cells were then stained with PI solution containing RNase A to degrade RNA, followed by incubation for 30 min at 37°C. Flow cytometric analysis was conducted to determine the distribution of cells in different phases of the cell cycle (G0/G1, S, and G2/M). Data were collected using an Attune™ NxT Flow Cytometer (Thermo Fisher Scientific Inc., Waltham, MA, USA), and the percentage of cells in each phase was calculated using FlowJo software. Experiments were repeated in triplicate to ensure statistical reliability.

Statistical analysis

The data from triplicate repetitions for each experiment was taken to maintain reproducibility and was revealed as±SD. Data analysis and student *t*-test execution were conducted using Origin Pro software, which was followed by a two-way ANOVA. The thresholds for statistical significance were *p* values below 0.05 and 0.01.

RESULTS

The drug-likeness characteristics for kaempferol

The complete study design and methodology adopted for the current research work are depicted in Figure 1. Kaempferol has advantageous drug-likeness characteristics (Table S1), indicating its potential as a therapeutic agent, with a molecular weight of 286.24 g/mol, fulfilling the requirements of a drug candidate. A consensus Log *p* value of 1.58 indicates a moderate degree of lipophilicity, influencing its solubility and bioavailability. The molecule has one flexible bond, which makes it more rigid, and it has six sites that can accept hydrogen bonds and four

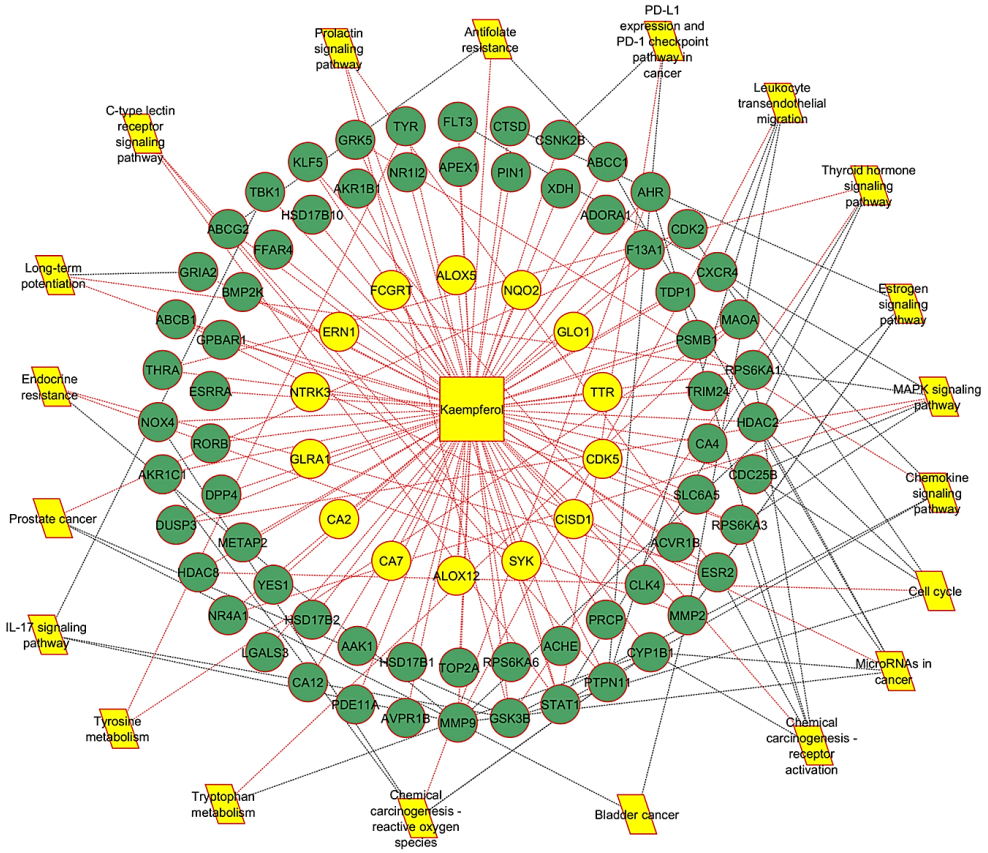

Figure 2: Comprehensive network linking kaempferol's hub genes and KEGG-enriched pathways relevant to liver cancer, demonstrating its multidimensional therapeutic potential.

sites that can donate hydrogen bonds, allowing it to interact well with biological targets. The TPSA of 111.13 Å² exhibited excellent hydrogen-bonding capacity, which compensates for its better gastrointestinal absorption characteristics. Kaempferol is water-soluble and has a bioavailability score of 0.55, indicating its potential for oral absorption. Significantly, it does not traverse the blood-brain barrier, thereby reducing the likelihood of adverse effects on the central nervous system. The druglikeness characteristics of kaempferol were also visualized with a radar plot obtained from SwissADME server (Figure S1). It has a non-toxic profile, as it does not exhibit hepatotoxicity, neurotoxicity, cytotoxicity, cardiotoxicity, or nephrotoxicity, rendering it sufficiently safe for therapeutic uses (Table S1). These qualities demonstrate that kaempferol satisfies the requirements for druglikeness, making it a prospective agent that may be regarded as both safe and effective.

Kaempferol-associated biological targets and their intersection with liver cancer

The use of Superpred and SwissTargetPrediction servers allowed for the confirmation of 80 biological targets for kaempferol (Supplementary Table S2). Figure S2-A shows that the targets predicted by SwissTarget Prediction belonged to several classifications. With a GIFTS score filter of 55 and higher, 3936 disease targets for liver cancer (Supplementary Table S3) were predicted using Genecards. There were 70 genes that overlapped or intersected with the kaempferol-associated biological targets (Supplementary Table S4) (Figure S2-B).

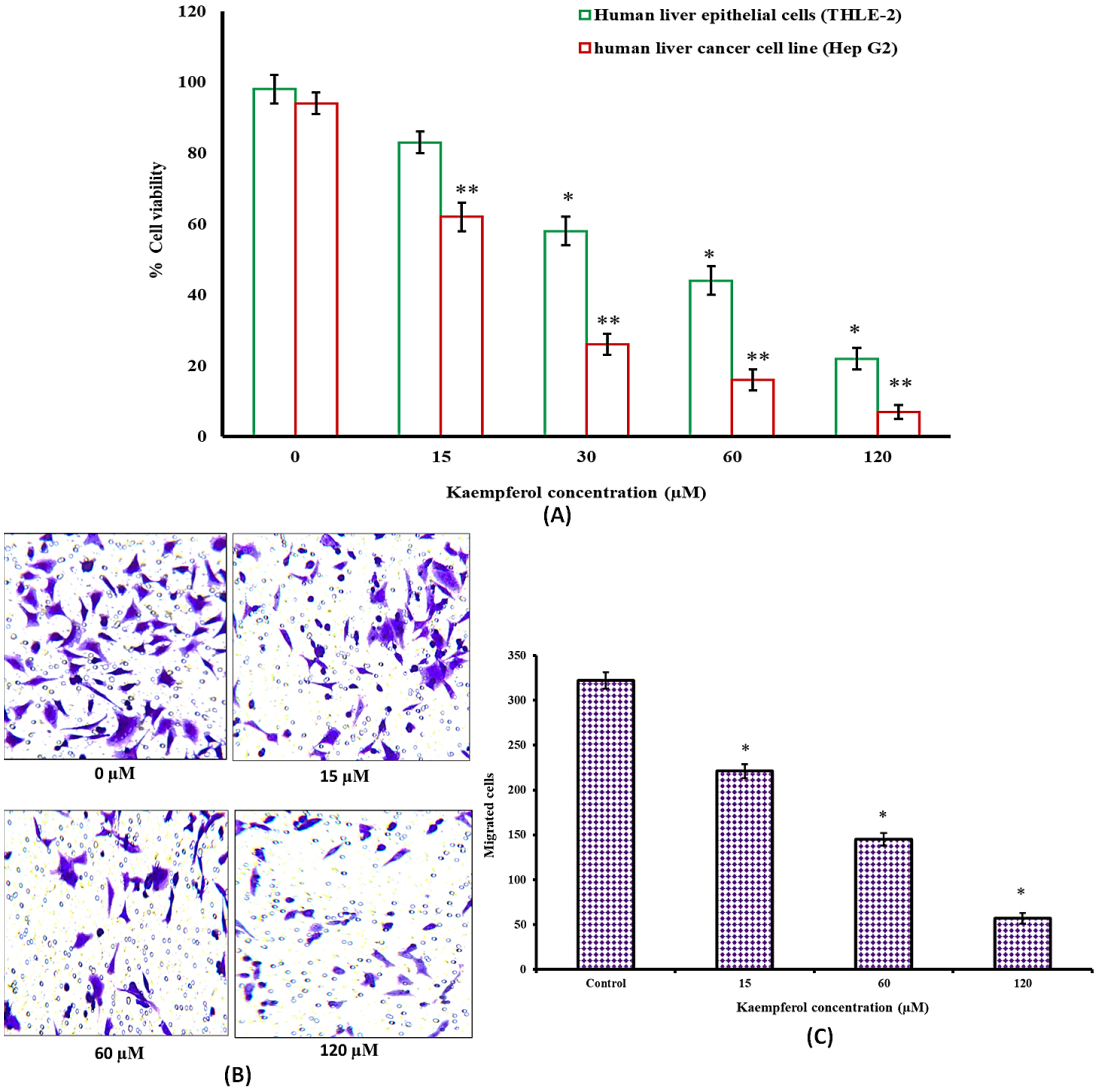

Figure 3: (A) Cytotoxic effects of kaempferol on HEP-G2 cells, showing a dose-dependent reduction in viability, with significant cytotoxicity observed at 60 µM and 120 µM compared to controls. (B) Transwell migration assay demonstrating reduced migratory capacity of HEP-G2 cells upon treatment with kaempferol at 60 and 120 µM, with fewer cells traversing the membrane. (C) Microscopic analysis of kaempferol-treated HEP-G2 cells, revealing reduced cell adherence and clustering, consistent with decreased migratory potential at higher concentrations. The data was shown as ±SD and the statistical significance was set at *p<0.05 and **p<0.01.

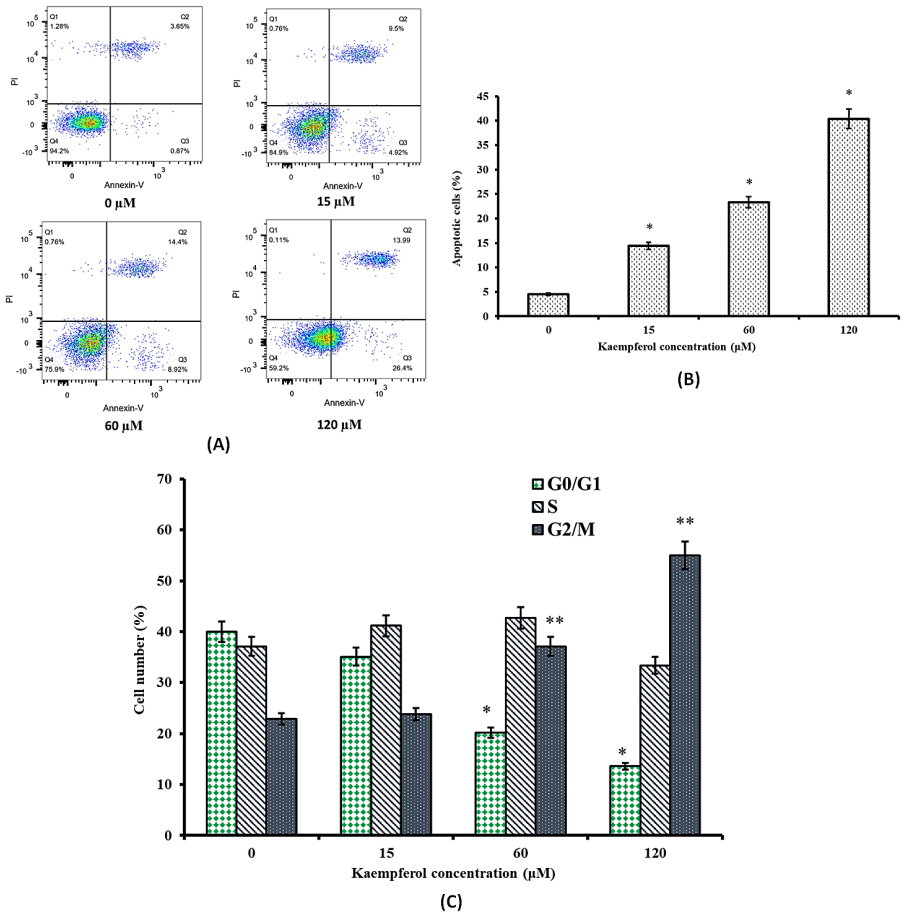

Figure 4: (A) Flow cytometric analysis of apoptosis in HEP-G2 cells treated with kaempferol, showing increased apoptotic populations at 15, 60, and 120 µM concentrations. (B) Detailed apoptosis data showing predominantly early and late apoptotic populations in kaempferol-treated cells, with negligible necrotic effects, confirming its pro-apoptotic mode of action. (C) Cell cycle analysis of HEP-G2 cells treated with kaempferol, showing dose-dependent arrest at the G2/M phase, indicating disruption of mitotic progression and inhibition of proliferation. The data was shown as ±SD and the statistical significance was set at *p<0.05 and **p<0.01.

PPI Network and hub targets for kaempferol

Seventy overlapping genes were mapped into the STRING database to form the PPI network, as seen in Figure S3-A. Cytoscape was used to assess the created network, with statistical values presented in Figure S3-B. The structure had 70 nodes interconnected by 154 edges, resulting in an average node degree of 4.4 and an average local clustering coefficient of 0.428. The high significance of the PPI enrichment p-value (<1.0e-16) suggests a significant degree of functional connectivity between these genes when compared to the expected edge count for a random network (65). Significant hub genes with notable connections, such as GSK3B, MMP9, and STAT1, were identified as essential regulators within the network and are emphasised in Figure S3-C. These results underscore the biological significance of these genes in the fundamental processes, indicating their potential as therapeutic or diagnostic targets.

Kaempferol associated hub targets gene-ontology and enrichment pathways

The functional enrichment analysis highlights several key BP, CC and MF, and pathways associated with kaempferol and its hub targets, particularly in the context of liver cancer.

BP: Kaempferol influences pathways involved in the positive regulation of smooth muscle cell proliferation, protein autophosphorylation, and the cellular response to peptides and amyloid-beta. It modulates processes such as the regulation of MAP kinase activity, including its positive regulation, and impacts the intracellular receptor signaling pathway and icosanoid metabolic processes (Figure S4-A).

CC: The targets of kaempferol localize to diverse cellular structures, including the ficolin-1-rich granule lumen, serine/threonine protein kinase complexes, and the external side of the plasma membrane. Other significant components include the apical plasma membrane, secretory granule lumen, and

cytoplasmic vesicle lumen, emphasizing its involvement in vesicular and membrane-related processes (Figure S4-B).

MF: Kaempferol exhibits activity in nuclear receptor activation, ligand-activated transcription factor binding, and protein serine/threonine kinase activity. Additionally, it engages in RNA polymerase II-specific transcription factor binding, heat shock protein binding, and efflux transmembrane transporter activity, underscoring its regulatory and protective roles at the molecular level (Figure S4-C).

KEGG Pathways: Enriched pathways include pivotal signaling networks such as the chemokine signaling pathway, C-type lectin receptor signaling, and MAPK signaling pathway, along with metabolic routes like tryptophan and tyrosine metabolism. Kaempferol's association with cancer-specific pathways, such as PD-L1 expression and PD-1 checkpoint regulation, IL-17 signaling, microRNAs in cancer, and chemical carcinogenesis, further demonstrates its therapeutic potential. It also plays a role in endocrine-related pathways, including estrogen and prolactin signaling, and cell cycle regulation (Figure S5).

A consolidated network linking kaempferol, its hub targets, and these KEGG-enriched pathways in liver cancer is presented in Figure 2, showcasing its multidimensional regulatory effects and therapeutic relevance.

Expression analysis for kaempferol associated hub targets in liver cancer

Analysis using GEPIA2 revealed distinct expression patterns for GSK3B, MMP9, and STAT1 in tumor and normal tissues. GSK3B exhibited elevated expression in tumor tissues (Figure S6-A), with levels remaining consistently high across stages I-III, followed by a marked reduction at stage IV, as shown in the violin plot (F value=2.01; Pr (>F)=0.113) (Figure S6-B). Survival analysis showed that patients had better outcomes when GSK3B levels were lower, as seen in the Kaplan-Meier plots (Figure S6-C). For MMP9, expression was significantly higher in tumor tissues than in normal samples (Figure S7-A). Stage-specific analysis revealed a pronounced increase from stage I to II, followed by moderate rises from II to III and III to IV (F value=1.45; Pr (>F)=0.22) (Figure S7-B). Lower MMP9 expression correlated with improved survival rates (Figure S7-C). STAT1 demonstrated increased expression in tumor tissues (Figure S8-A) but showed a progressive decline from stage I to stage IV (F value = 1.32; Pr (>F)=0.26) (Figure S8-B). Survival analysis revealed a complex relationship, as both low and high STAT1 expression levels were variably associated with patient outcomes (Figure S8-C).

Kaempferol targeted hub genes in TME

The TIMER results illustrated the correlation between the expression levels of GSK3B, MMP9, and STAT1 (log2 TPM) and immune infiltration levels in liver hepatocellular carcinoma. GSK3B showed a positive strong association with immune cells, particularly CD4+T cells, neutrophils, and macrophages, indicating its role in both adaptive and innate immune processes (Figure S9). MMP9 is negatively strongly associated with B cells, macrophages, and dendritic cells, suggesting its role in immune cell recruitment and response regulation (Figure S9**)**. STAT1 displayed significant associations with B cells, dendritic cells, CD8+T cells, and neutrophils, highlighting its involvement in modulating adaptive and innate immunity (Figure S9). Collectively, these genes influence immune dynamics in the tumor microenvironment.

Hub gene verification and interactions with Kaempferol using Molecular Docking and Dynamics

The docking results for kaempferol with GSK3B, MMP9, and STAT1 indicate notable interactions with varying binding affinities and structural characteristics (Table S5). Kaempferol demonstrated the strongest binding affinity with MMP9 (Vina score: -9.2 kcal/mol), followed by GSK3B (-8.9 kcal/mol) and STAT1 (-7 kcal/mol) (Figure S10). These differences reflect distinct receptor-ligand interactions and binding efficiencies. The docking site cavity volumes also varied, with GSK3B having the largest cavity (889 $Å^3$), indicating more space for ligand accommodation, followed by STAT1 (709 $Å^3$) and MMP9 (585 $Å^3$). The docking centers and sizes were specific for each receptor, reflecting their unique spatial configurations. Furthermore, kaempferol exhibited diverse interactions, including hydrogen bonds, hydrophobic contacts, and possibly π-π stacking, tailored to the binding sites of each receptor. These findings display the versatility of kaempferol in targeting multiple proteins with differing structural and interaction profiles. The interacting residues and binding interaction types are shown in Figure S10.

The deformability and beta factors (B-factors) of the docked complexes of kaempferol with GSK3B (Figure S11-A), MMP9 (Figure S11-B), and STAT1 (Figure S11-C) provide critical insights into their flexibility and stability (Figure S11). Deformability measures the extent of flexibility for each residue within the protein, and in these complexes, regions such as loops and turns typically exhibit higher peaks in the deformability graph, indicating significant movement potential. These regions may correspond to flexible domains or hinge points near the ligand-binding site, enabling conformational adjustments to accommodate kaempferol. Conversely, more rigid areas, such as secondary structural elements like α-helices and β-sheets, display minimal deformability, contributing to the structural integrity of the protein. Beta factors further corroborate these findings by quantifying atomic displacement or mobility. Higher B-factors, observed in flexible regions, suggest dynamic movements that could facilitate ligand interactions or signal transduction. In contrast, lower B-factors in the rigid core regions of the protein confirm their role in maintaining overall stability. Among the complexes, variations in deformability and beta factors may reflect differences in the structural adaptability of GSK3B, MMP9,

and STAT1 upon binding kaempferol, emphasizing the interplay between ligand binding and protein dynamics in biological systems.

Kaempferol mediated cytotoxicity

Kaempferol reduced HEP-G2 cell viability in a concentration-dependent manner. At 15 µM, minimal reduction in cell survival was observed, while significant cytotoxicity was evident at 60 and 120 µM. Compared to the results from HEP-G2 cells, the THLE-2 cells showed higher cell survival (Figure 3A). This showed selectivity in the antiproliferative efficacy of kaempferol against the HEP-G2 cells sparing the normal cells. The IC_{50} values with respect to the cancerous and normal cells were found to be 24.5 µM and 58.1 µM respectively.

Kaempferol targeting cellular migration

Kaempferol inhibited HEP-G2 cell migration significantly at concentrations of 60 and 120 µM. Fewer cells traversed the Transwell membrane compared to untreated controls (Figure 3B). At 15 µM, a modest decrease in migration was observed (Figure 3C). Microscopic analysis revealed a reduction in cell clustering and adherence at higher concentrations, correlating with suppressed migratory capacity.

Kaempferol triggers apoptosis in HEP-G2 cells

Flow cytometric analysis showed a marked increase in apoptotic cell populations with increasing kaempferol concentrations (Figure 4A). Early apoptosis was evident at 15 µM, while 60 and 120 µM induced both early and late apoptosis. The percentage of necrotic cells remained low, suggesting the pro-apoptotic efficacy of kaempferol, rather than necrotic, mode of action (Figure 4B). Untreated cells maintained a predominantly viable population, confirming the targeted approach of kaempferol.

G2/M phase arrest by Kaempferol in HEP-G2 cells

Kaempferol caused significant cell cycle arrest in HEP-G2 cells, predominantly at the G2/M phase. This effect was dose-dependent, with 60 and 120 µM treatments showing the highest percentage of cells arrested in the G2/M phase (Figure 4C). A corresponding decrease in the S and G0/G1 phase population was observed, indicating reduced DNA synthesis and proliferation. Untreated cells showed a typical cell cycle distribution, confirming the specificity of kaempferol action.

DISCUSSION

The network pharmacology approach identified GSK3B, MMP9, and STAT1 as hub genes closely associated with biological activities of kaempferol. These genes were evaluated in the context of their roles in Gene Ontology (GO), KEGG Pathways, Expression Profiles (GEPIA2), Tumor Microenvironment Interactions (TIMER), molecular docking, dynamics, and their impact on cellular processes such as cytotoxicity, migration, apoptosis, and the cell cycle. The comprehensive insights provided by these analyses highlight the multifaceted therapeutic potential of kaempferol.

Glycogen Synthase Kinase 3 beta (GSK3B) is a serine/threonine kinase involved in various cellular processes, including cell survival, apoptosis, and proliferation.[26-28] GO enrichment analysis revealed that GSK3B is implicated in pathways such as protein autophosphorylation and MAP kinase activity regulation, emphasizing its role in intracellular signaling. KEGG pathway enrichment indicated its involvement in cancer-specific pathways like the Wnt signaling pathway, PI3K-Akt signaling, and chemokine signaling, all of which are critical for tumorigenesis. GEPIA2 analysis showed that GSK3B is significantly upregulated in liver cancer tissues compared to normal tissues, with consistent expression across early cancer stages (I-III) and a decrease at stage IV. TIMER analysis demonstrated a strong positive correlation between GSK3B expression and immune infiltration of CD4+T cells, neutrophils, and macrophages, indicating its role in modulating the tumor microenvironment.[29] Molecular docking showed a high binding affinity of kaempferol to GSK3B, with a Vina score of -8.9 kcal/mol and interactions mediated by hydrogen bonds and hydrophobic contacts. Dynamics analysis further supported the stability of this interaction, with GSK3B exhibiting moderate flexibility near the ligand-binding site. Experimentally, kaempferol exhibited significant cytotoxicity against HEP-G2 cells in a dose-dependent manner, with higher concentrations showing more pronounced effects. This cytotoxicity correlated with ability of kaempferol to reduce cell migration, as seen in Transwell assays. Furthermore, kaempferol induced G2/M phase arrest in cell cycle studies, disrupting mitotic progression. The pro-apoptotic effects of kaempferol, evident from flow cytometry, may also be partly mediated through GSK3B modulation, making it a critical therapeutic target.[30]

Matrix Metalloproteinase 9 (MMP9) is a key enzyme involved in extracellular matrix remodeling, which is essential for tumor invasion and metastasis.[31,32] GO analysis highlighted its association with biological processes such as positive regulation of smooth muscle cell proliferation and cellular response to amyloid-beta. KEGG enrichment linked MMP9 to pathways like ECM-receptor interaction, cytokine-cytokine receptor interaction, and MAPK signaling, underscoring its relevance in cancer progression.[33] MMP9 expression was markedly elevated in liver cancer tissues compared to normal samples, as per GEPIA2 analysis, and increased progressively from stage I to IV. TIMER analysis revealed that MMP9 negatively correlated with immune cell populations such as B cells and dendritic cells, suggesting a role in evading immune surveillance.[34] Molecular docking results showed strong binding affinity of kaempferol for MMP9, with a Vina score of -9.2 kcal/mol and interactions involving key residues. Molecular dynamics confirmed the stability of this interaction, with MMP9 demonstrating localized flexibility near

the binding pocket. Kaempferol effects on MMP9 were reflected in its ability to inhibit HEP-G2 cell migration significantly at higher concentrations, reducing metastatic potential. Cytotoxicity assay revealed a dose-dependent reduction in cell viability, with selective toxicity against cancer cells. Apoptosis assays further showed that kaempferol induced both early and late apoptosis in a dose-dependent manner, potentially mediated through MMP9 modulation. Additionally, kaempferol effects on cell cycle regulation included an increase in the G2/M phase population, highlighting its role in arresting cell division. These findings position MMP9 as a pivotal target in anti-cancer activity of Kaempferol.

Signal Transducer and Activator of Transcription 1 (STAT1) plays a dual role in cancer, acting as both a tumor suppressor and a pro-tumorigenic factor, depending on the context.[35-37] GO analysis identified STAT1's involvement in processes like nuclear receptor activity and ligand-activated transcription factor binding. KEGG pathway enrichment linked STAT1 to pathways such as cytokine signaling, IL-17 signaling, and cancer-related signaling, highlighting its diverse functional roles. GEPIA2 analysis showed increased STAT1 expression in tumor tissues compared to normal tissues, with a gradual decline from stage I to IV. This trend may reflect changes in STAT1's role during tumor progression. TIMER analysis revealed significant correlations between STAT1 expression and immune cell infiltration, including B cells, dendritic cells, and neutrophils, suggesting its involvement in shaping the immune microenvironment. Docking studies showed a moderate binding affinity of kaempferol to STAT1 (Vina score: -7 kcal/mol), with key hydrogen bond interactions. Molecular dynamics analysis indicated that STAT1's binding site exhibited higher flexibility, enabling dynamic interactions with kaempferol. Experimentally, kaempferol targeting of STAT1 was associated with a dose-dependent increase in cytotoxicity, apoptosis, and cell cycle arrest at the G2/M phase in HEP-G2 cells. These effects suggest that STAT1 may play a role in mediating ability of kaempferol to induce cell death and suppress proliferation. Additionally, kaempferol inhibited cellular migration, further reducing the metastatic potential of liver cancer cells. STAT1's influence on immune cell dynamics highlights its potential as a target for immunomodulatory therapy.[38-40]

Our findings align with previously reported pharmacological and mechanistic actions of kaempferol observed across various cancer models.[41] Kaempferol exhibits potent anticancer effects across multiple tumor types by modulating key signaling pathways, including GSK3β, MMP9, and STAT1. In gastric cancer, it suppresses the AKT/GSK3β pathway, leading to reduced GSK3β phosphorylation and inhibition of Epithelial-Mesenchymal Transition (EMT), thereby limiting tumor invasion and metastasis.[42] In breast cancer (MCF-7, MDA-MB-231) and osteosarcoma (143B, U2OS), kaempferol downregulates MMP9 expression and activity, impairing extracellular matrix degradation and cell migration.[43] Additionally, in hepatocellular carcinoma (HepG2, Huh-7, SK-HEP-1) and non-small cell lung cancer (A549), kaempferol modulates STAT1 signaling by enhancing STAT1/2 activity while inhibiting STAT3 and PI3K/AKT/mTOR, promoting apoptosis and cell-cycle arrest.[44] By focusing on hub genes GSK3B, MMP9, and STAT1 and corroborating their predicted interactions through dynamic simulations and functional assays, we offer a more mechanistically precise and livercancer-specific evaluation than previous studies that predominantly relied on isolated pathway analyses or single-method approaches.

CONCLUSION

In conclusion, this study highlights multi-targeted therapeutic potential of kaempferol against liver cancer by an integrated approach that combines experimental validation and network pharmacology. The main liver cancer-related targets, GSK3B, MMP9, and STAT1, which are implicated in significant signalling cascades such Wnt, PI3K-Akt, and ECM-receptor interaction, showed strong binding affinities and persistent interactions with kaempferol. Analysis of expression and functional enrichment further supported the importance of these targets in hepatocarcinogenesis. The *in vitro* biochemical assays revealed dose-dependent suppression of HEP-G2 cell migration, proliferation, early and late apoptosis, and G2/M phase cell cycle arrest was imparted by Kaempferol in HEP-G2 cells. These findings indicate that kaempferol is a promising, low-toxicity pharmacological agent for liver cancer treatment and call for further preclinical and clinical research.

ACKNOWLEDGEMENT

Not applicable.

CONFLICT OF INTEREST

The authors declare that there is no conflict of interest.

ABBREVIATIONS

ADME: Absorption, Distribution, Metabolism, and Excretion; **ANOVA**: Analysis of Variance; **DMEM:** Dulbecco's Modified Eagle Medium; **DMSO:** Dimethyl Sulfoxide; **ECM:** Extracellular Matrix; **FBS:** Fetal Bovine Serum; **FITC:** Fluorescein Isothiocyanate; **GEPIA2:** Gene Expression Profiling Interactive Analysis 2; **GO:** Gene Ontology; **GSK3B:** Glycogen Synthase Kinase 3 Beta; **GTEx:** Genotype-Tissue Expression; **HEP-G2:** Human Hepatocellular Carcinoma Cell Line; **IL-17:** Interleukin-17; **KEGG:** Kyoto Encyclopedia of Genes and Genomes; **MAPK:** Mitogen-Activated Protein Kinase; **MMP9:** Matrix Metalloproteinase 9; **MTT:** 3-(4,5-Dimethylthiazol-2-yl)-2,5-diphenyltetrazolium bromide; **PBS:** Phosphate-Buffered Saline; **PI:** Propidium Iodide; **PI3K :** Phosphoinositide 3-Kinase; **PPI:** Protein-Protein Interaction; **STAT1:** Signal Transducer and

Activator of Transcription 1; **TCGA:** The Cancer Genome Atlas; **TIMER:** Tumor Immune Estimation Resource; **TME** - Tumor Microenvironment.

SUMMARY

Kaempferol has promising drug-like characteristics, meeting essential criteria for therapeutic use. The molecular weight of 286.24 g/mol and a Log P value of 1.58 indicate moderate lipophilicity, affecting solubility and bioavailability. It comprises one rotatable bond, six hydrogen bond acceptors, and four hydrogen bond donors, which contribute to structural stability and possible biological interactions. A TPSA of 111.13 Å² facilitates effective hydrogen bonding, enabling substantial gastrointestinal absorption. The water solubility and a bioavailability value of 0.55 indicate its potential for oral absorption. Kaempferol cannot penetrate the Blood-Brain Barrier (BBB), hence mitigating central nervous system hazards, and has a non-toxic profile devoid of hepatotoxicity, neurotoxicity, cytotoxicity, cardiotoxicity, or nephrotoxicity. SuperPred and SwissTargetPrediction identified 80 biological targets, 70 of which coincided with liver cancer targets in Genecards. STRING-based PPI network analysis revealed 70 nodes and 154 edges, highlighting the key hub genes GSK3B, MMP9, and STAT1. Functional enrichment study linked kaempferol to pathways including MAPK signaling, chemokine signaling, and PD-L1 checkpoint regulation. Expression analysis (GEPIA2) indicated upregulation of GSK3B and MMP9 in liver cancer, whereas survival analysis demonstrated that reduced expression correlates with improved prognosis. TIMER analysis indicated a strong association between GSK3B and immune cells, a negative correlation between MMP9 and immune recruitment, and the role of STAT1 in adaptive immunity. Molecular docking confirmed kaempferol's significant binding affinity for MMP9 (-9.2 kcal/mol), GSK3B (-8.9 kcal/mol), and STAT1 (-7 kcal/mol). Kaempferol elicited cytotoxicity in HEP-G2 cells while sparing normal cells. Kaempferol inhibited cell migration, promoted apoptosis, and caused G2/M cell cycle arrest. The multifaceted anticancer efficacy of kaempferol via apoptosis induction, cell cycle control, and interactions with the immunological microenvironment underscores its promise for liver cancer therapy.

REFERENCES

1. Zhang CH, Cheng Y, Zhang S, Fan J, Gao Q. Changing epidemiology of hepatocellular carcinoma in Asia. Liver Int. 2022; 42(9): 2029-41. doi: 10.1111/liv.15251, PMID 35319165.
2. Li Q, Cao M, Lei L, Yang F, Li H, Yan X, *et al.* Burden of liver cancer: from epidemiology to prevention. Chin J Cancer Res. 2022; 34(6): 554-66. doi: 10.21147/j.issn.1000-9604.2022.06.02, PMID 36714347.
3. Cha DI, Lee MW, Hyun D, Ahn SH, Jeong WK, Rhim H. Combined transarterial chemoembolization and radiofrequency ablation for hepatocellular carcinoma infeasible for ultrasound-guided percutaneous radiofrequency ablation: A comparative study with general ultrasound-guided radiofrequency ablation outcomes. Cancers. 2023; 15(21): 5193. doi: 10.3390/cancers15215193, PMID 37958370.
4. Chow R, Simone CB, Jairam MP, Swaminath A, Boldt G, Lock M. Radiofrequency ablation vs radiation therapy vs transarterial chemoembolization vs yttrium 90 for local treatment of liver cancer-a systematic review and network meta-analysis of survival data. Acta Oncol. 2022; 61(4): 484-94. doi: 10.1080/0284186X.2021.2009563, PMID 34846988.
5. Weber M, Lam M, Chiesa C, Konijnenberg M, Cremonesi M, Flamen P, *et al.* EANM procedure guideline for the treatment of liver cancer and liver metastases with intra-arterial radioactive compounds. Eur J Nucl Med Mol Imaging. 2022; 49(5): 1682-99. doi: 10.1007/s00259-021-05600-z, PMID 35146577.
6. Man S, Luo C, Yan M, Zhao G, Ma L, Gao W. Treatment for liver cancer: from sorafenib to natural products. Eur J Med Chem. 2021; 224: 113690. doi: 10.1016/j.ejmech.2021.113690, PMID 34256124.
7. Fărcaș A, Drețcanu G, Pop TD, Enaru B, Socaci S, Diaconeasa Z. Cereal processing by-products as rich sources of phenolic compounds and their potential bioactivities. Nutrients. 2021; 13(11): 3934. doi: 10.3390/nu13113934, PMID 34836189.
8. Bangar SP, Chaudhary V, Sharma N, Bansal V, Ozogul F, Lorenzo JM. Kaempferol: A flavonoid with wider biological activities and its applications. Crit Rev Food Sci Nutr. 2023; 63(28): 9580-604. doi: 10.1080/10408398.2022.2067121, PMID 35468008.
9. Alam W, Khan H, Shah MA, Cauli O, Saso L. Kaempferol as a dietary anti-inflammatory agent: current therapeutic standing. Molecules. 2020; 25(18): 4073. doi: 10.3390/molecules25184073, PMID 32906577.
10. Fouzder C, Mukhuty A, Kundu R. Kaempferol inhibits Nrf2 signalling pathway via downregulation of Nrf2 mRNA and induces apoptosis in NSCLC cells. Arch Biochem Biophys. 2021; 697: 108700. doi: 10.1016/j.abb.2020.108700, PMID 33271149.
11. Alam MS, Sultana A, Sun H, Wu J, Guo F, Li Q, *et al.* Bioinformatics and network-based screening and discovery of potential molecular targets and small molecular drugs for breast cancer. Front Pharmacol. 2022; 13: 942126. doi: 10.3389/fphar.2022.942126, PMID 36204232.
12. Batool S, Javed MR, Aslam S, Noor F, Javed HM, Seemab R, *et al.* Network pharmacology and bioinformatics approach reveals the multi-target pharmacological mechanism of *Fumaria indica* in the treatment of liver cancer. Pharmaceuticals (Basel). 2022; 15(6): 654. doi: 10.3390/ph15060654, PMID 35745580.
13. Kawsar SM, Munia NS, Saha S, Ozeki Y. *In silico* pharmacokinetics, molecular docking and molecular dynamics simulation studies of nucleoside analogs for drug discovery-a mini review. Mini Rev Med Chem. 2024; 24(11): 1070-88. doi: 10.2174/0113895575258033231024073521, PMID 37957918.
14. Somda D, Kpordze SW, Jerpkorir M, Mahora MC, Ndungu JW, Kamau SW, *et al.* The role of bioinformatics in drug discovery: A comprehensive overview. Drug Metabolism and Pharmacokinetics; 2023.
15. Daina A, Michielin O, Zoete V. SwissADME: a free web tool to evaluate pharmacokinetics, drug-likeness and medicinal chemistry friendliness of small molecules. Sci Rep. 2017; 7(1): 42717. doi: 10.1038/srep42717, PMID 28256516.
16. Banerjee P, Kemmler E, Dunkel M, Preissner R. ProTox 3.0: a webserver for the prediction of toxicity of chemicals. Nucleic Acids Res. 2024; 52(W1):W513-20. doi: 10.1093/nar/gkae303, PMID 38647086.
17. Gallo K, Goede A, Preissner R, Gohlke BO. SuperPred 3.0: drug classification and target prediction-a machine learning approach. Nucleic Acids Res. 2022; 50(W1):W726-31. doi: 10.1093/nar/gkac297, PMID 35524552.
18. Daina A, Michielin O, Zoete V. SwissTargetPrediction. SwissTargetPrediction: updated data and new features for efficient prediction of protein targets of small molecules. Nucleic Acids Res. 2019; 47(W1):W357-64. doi: 10.1093/nar/gkz382, PMID 31106366.
19. Safran M, Rosen N, Twik M, BarShir R, Stein TI, Dahary D, *et al.* The genecards suite. Practical guide to life science databases; 2021. p. 27-56.
20. Bardou P, Mariette J, Escudié F, Djemiel C, Klopp C. jvenn: an interactive Venn diagram viewer. BMC Bioinformatics. 2014; 15(1): 293. doi: 10.1186/1471-2105-15-293, PMID 25176396.
21. Szklarczyk D, Kirsch R, Koutrouli M, Nastou K, Mehryary F, Hachilif R, *et al.* The STRING database in 2023: protein-protein association networks and functional enrichment analyses for any sequenced genome of interest. Nucleic Acids Res. 2023; 51(D1):D638-46. doi: 10.1093/nar/gkac1000, PMID 36370105.
22. Ge SX, Jung D, Yao R. ShinyGO: a graphical gene-set enrichment tool for animals and plants. Bioinformatics. 2020; 36(8): 2628-9. doi: 10.1093/bioinformatics/btz931, PMID 31882993.
23. Tang Z, Kang B, Li C, Chen T, Zhang Z. GEPIA2: an enhanced web server for large-scale expression profiling and interactive analysis. Nucleic Acids Res. 2019; 47(W1):W556-60. doi: 10.1093/nar/gkz430, PMID 31114875.
24. Li T, Fan J, Wang B, Traugh N, Chen Q, Liu JS, *et al.* TIMER: a web server for comprehensive analysis of tumor-infiltrating immune cells. Cancer Res. 2017; 77(21): e108-10. doi: 10.1158/0008-5472.CAN-17-0307, PMID 29092952.
25. Liu Y, Yang X, Gan J, Chen S, Xiao ZX, Cao Y. CB-Dock2: improved protein-ligand blind docking by integrating cavity detection, docking and homologous template fitting. Nucleic Acids Res. 2022; 50(W1):W159-64. doi: 10.1093/nar/gkac394, PMID 35609983.
26. Duda P, Akula SM, Abrams SL, Steelman LS, Martelli AM, Cocco L, *et al.* Targeting GSK3 and associated signaling pathways involved in cancer. Cells. 2020; 9(5): 1110. doi: 10.3390/cells9051110, PMID 32365809.
27. Xu C, Du Z, Ren S, Pian Y. Downregulation of GSK3B by miR-132-3p enhances etoposide-induced breast cancer cell apoptosis. Ann Clin Lab Sci. 2021; 51(3): 285-94. PMID 34162557.
28. Taylan E, Zayou F, Murali R, Karlan BY, Pandol SJ, Edderkaoui M, *et al.* Dual targeting of GSK3B and HDACs reduces tumor growth and improves survival in an ovarian cancer

mouse model. Gynecol Oncol. 2020; 159(1): 277-84. doi: 10.1016/j.ygyno.2020.07.005, PMID 32698955.

29. Zheng X, Yang L, Shen X, Pan J, Chen Y, Chen J, *et al.* Targeting Gsk3a reverses immune evasion to enhance immunotherapy in hepatocellular carcinoma. J Immunother Cancer. 2024; 12(8): e009642. doi: 10.1136/jitc-2024-009642, PMID 39174053.
30. Lin J, Song T, Li C, Mao W. GSK-3β in DNA repair, apoptosis, and resistance of chemotherapy, radiotherapy of cancer. Biochim Biophys Acta Mol Cell Res. 2020; 1867(5): 118659. doi: 10.1016/j.bbamcr.2020.118659, PMID 31978503.
31. Augoff K, Hryniewicz-Jankowska A, Tabola R, Stach K. MMP9: a tough target for targeted therapy for cancer. Cancers. 2022; 14(7): 1847. doi: 10.3390/cancers14071847, PMID 35406619.
32. Mondal S, Adhikari N, Banerjee S, Amin SA, Jha T. Matrix metalloproteinase-9 (MMP-9) and its inhibitors in cancer: A minireview. Eur J Med Chem. 2020; 194: 112260. doi: 10.1016/j.ejmech.2020.112260, PMID 32224379.
33. Song Z, Wang J, Su Q, Luan M, Chen X, Xu X. The role of MMP-2 and MMP-9 in the metastasis and development of hypopharyngeal carcinoma. Braz J Orl. 2021; 87(5): 521-8. doi: 10.1016/j.bjorl.2019.10.009, PMID 31882379.
34. Buttacavoli M, Di Cara G, Roz E, Pucci-Minafra I, Feo S, Cancemi P. Integrated multi-omics investigations of metalloproteinases in colon cancer: focus on MMP2 and MMP9. Int J Mol Sci. 2021; 22(22): 12389. doi: 10.3390/ijms222212389, PMID 34830271.
35. Ji W, Peng Z, Sun B, Chen L, Zhang Q, Guo M, *et al.* LpCat1 promotes malignant transformation of hepatocellular carcinoma cells by directly suppressing STAT1. Front Oncol. 2021; 11: 678714. doi: 10.3389/fonc.2021.678714, PMID 34178664.
36. Zhou C, Liang T, Jiang J, Chen J, Chen T, Huang S, *et al.* MMP9 and STAT1 are biomarkers of the change in immune infiltration after anti-tuberculosis therapy, and the immune status can identify patients with spinal tuberculosis. Int Immunopharmacol. 2023; 116: 109588. doi: 10.1016/j.intimp.2022.109588, PMID 36773569.
37. Zhang J, Wang F, Liu F, Xu G. Predicting STAT1 as a prognostic marker in patients with solid cancer. Ther Adv Med Oncol. 2020; 12: 1758835920917558. doi: 10.1177/1758835920917558, PMID 32426049.
38. Zou S, Tong Q, Liu B, Huang W, Tian Y, Fu X. Targeting STAT3 in cancer immunotherapy. Mol Cancer. 2020; 19(1): 145. doi: 10.1186/s12943-020-01258-7, PMID 32972405.
39. Tanagala KK, Morin-Baxter J, Carvajal R, Cheema M, Dubey S, Nakagawa H, *et al.* SP140 inhibits STAT1 signaling, induces IFN-γ in tumor-associated macrophages, and is a predictive biomarker of immunotherapy response. J Immunother Cancer. 2022; 10(12): e005088. doi: 10.1136/jitc-2022-005088, PMID 36600652.
40. Wen Y, Ye S, Li Z, Zhang X, Liu C, Wu Y, *et al.* HDAC6 inhibitor ACY-1215 enhances STAT1 acetylation to block PD-L1 for colorectal cancer immunotherapy. Cancer Immunol Immunother. 2024; 73(1): 7. doi: 10.1007/s00262-023-03624-y, PMID 38231305.
41. Imran M, Salehi B, Sharifi-Rad J, Aslam Gondal T, Saeed F, Imran A, *et al*. Kaempferol: A key emphasis to its anticancer potential. Molecules. 2019; 24(12): 2277. doi: 10.3390/molecules24122277, PMID 31248102.
42. Gao XQ, Li HL, Wang M, Yang CT, Su R, Shao LH. Kaempferol inhibited invasion and metastasis of gastric cancer cells by targeting AKT/GSK3β pathway based on network pharmacology and molecular docking. J Asian Nat Prod Res. 2025; 27(3): 421-41. doi: 10.1080/10286020.2024.2387756, PMID 39132822.
43. Kaur S, Mendonca P, Soliman KF. The anticancer effects and therapeutic potential of kaempferol in triple-negative breast cancer. Nutrients. 2024; 16(15): 2392. doi: 10.3390/nu16152392, PMID 39125273.
44. Qattan MY, Khan MI, Alharbi SH, Verma AK, Al-Saeed FA, Abduallah AM, *et al.* Therapeutic importance of kaempferol in the treatment of cancer through the modulation of cell signalling pathways. Molecules. 2022; 27(24): 8864. doi: 10.3390/molecules27248864, PMID 36557997.

Cite this article: He Z, Liu W, Su N, Xing G. Decoding the Anticancer Mechanism of Action of Kaempferol in Liver Cancer Cells via Transcriptomics, Network Pharmacology, Molecular Docking, Dynamics Simulations, and *in vitro* Validation. Indian J of Pharmaceutical Education and Research. 2026;60(3):1206-17.

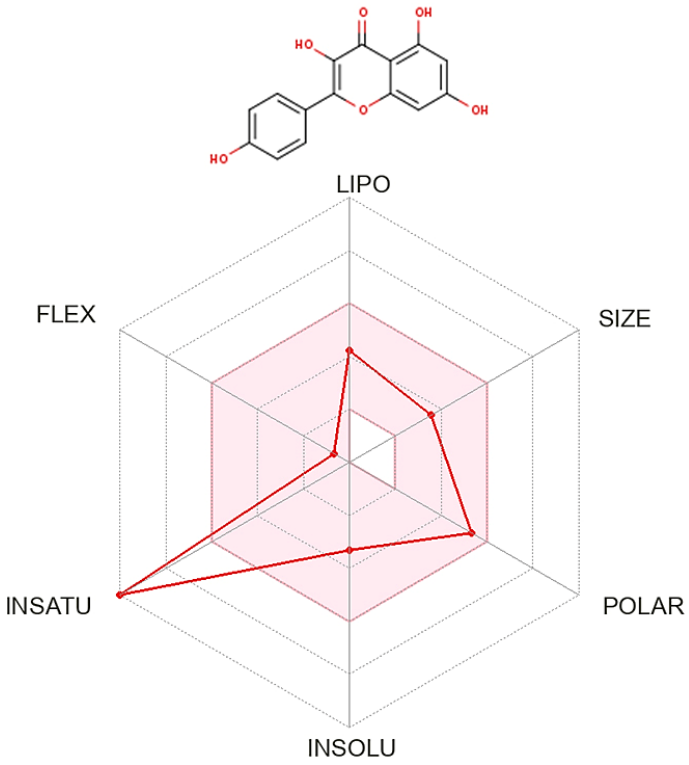

Figure S1: Radar plot visualizing the drug-likeness characteristics of kaempferol, derived from SwissADME analysis, highlighting its physicochemical properties such as lipophilicity and solubility. These properties indicate the suitability of kaempferol as a drug candidate.

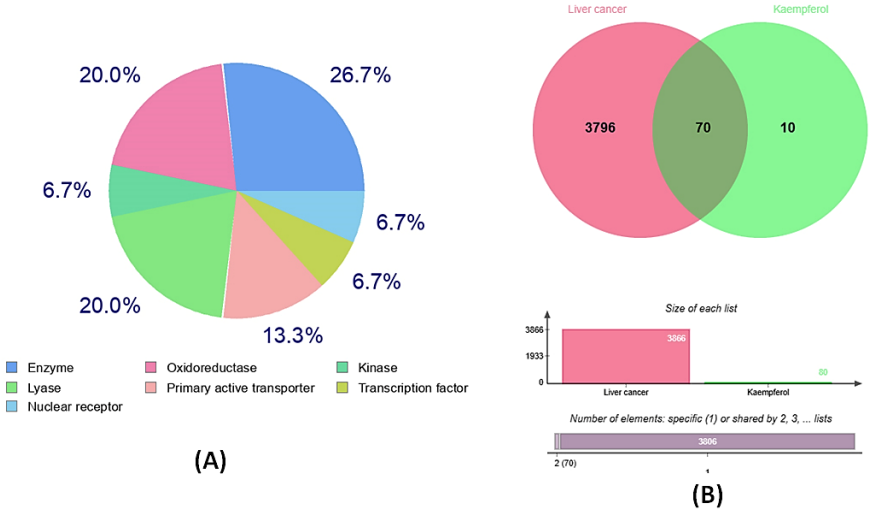

Figure S2: (A) Classification of kaempferol-associated biological targets predicted using the SwissTargetPrediction server, showing their diverse functional categories. (B) Venn diagram illustrating the overlap between 80 kaempferol-associated biological targets and 3,936 liver cancer-associated genes identified from GeneCards, with 70 genes intersecting as common targets.

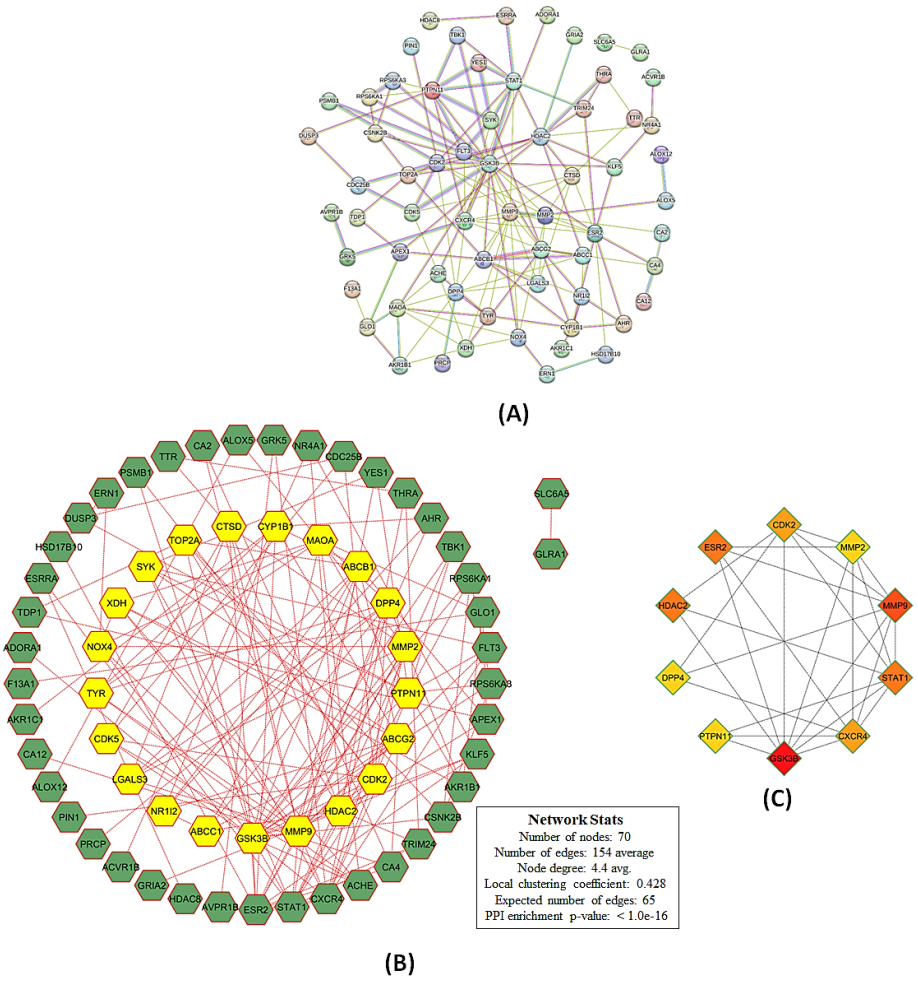

Figure S3: (A) Protein-Protein Interaction (PPI) network of 70 overlapping genes associated with kaempferol, constructed using STRING, illustrating functional relationships among the genes through nodes and edges. (B) Statistical analysis of the PPI network showing key metrics such as node degree, clustering coefficient, and enrichment p-values, demonstrating significant functional interconnections. (C) Identification of hub genes, including GSK3B, MMP9, and STAT1, as major regulators within the PPI network, with high connectivity and relevance in kaempferol's biological activity.

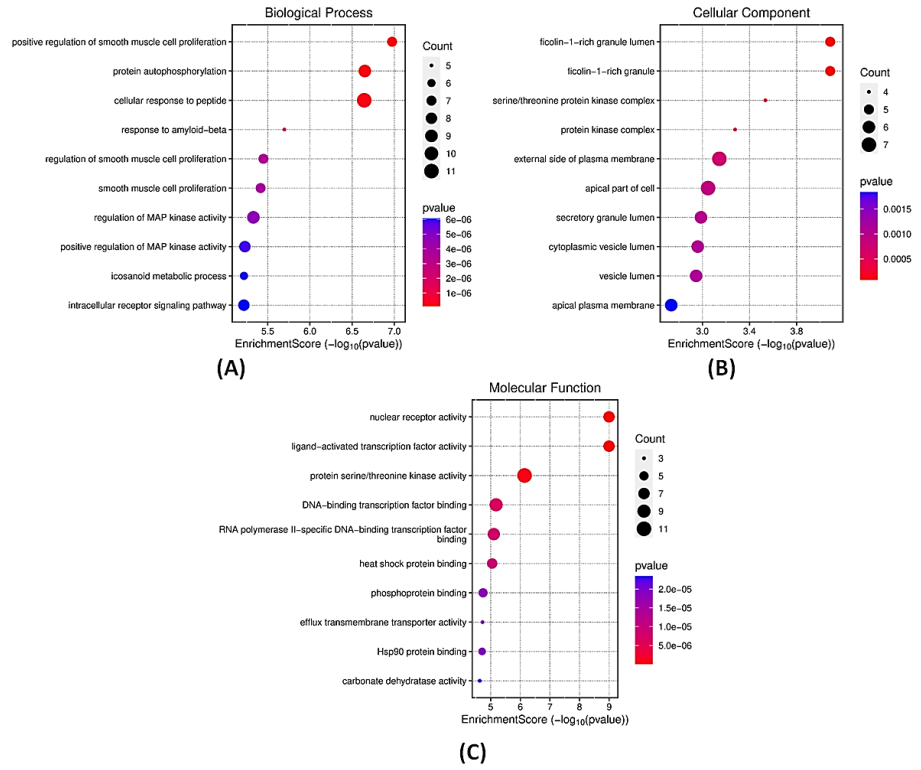

Figure S4: (A) Gene Ontology (GO) enrichment analysis of Biological Processes (BP) influenced by kaempferol's hub targets, emphasizing its role in pathways like smooth muscle cell proliferation, MAP kinase activity regulation, and peptide response. (B) GO enrichment of Cellular Components (CC) for kaempferol's hub targets, highlighting their localization to critical structures like plasma membranes, cytoplasmic vesicles, and secretory granules. (C) GO enrichment of Molecular Functions (MF) showing kaempferol's influence on activities such as nuclear receptor binding, protein kinase activity, and transcription factor interaction.

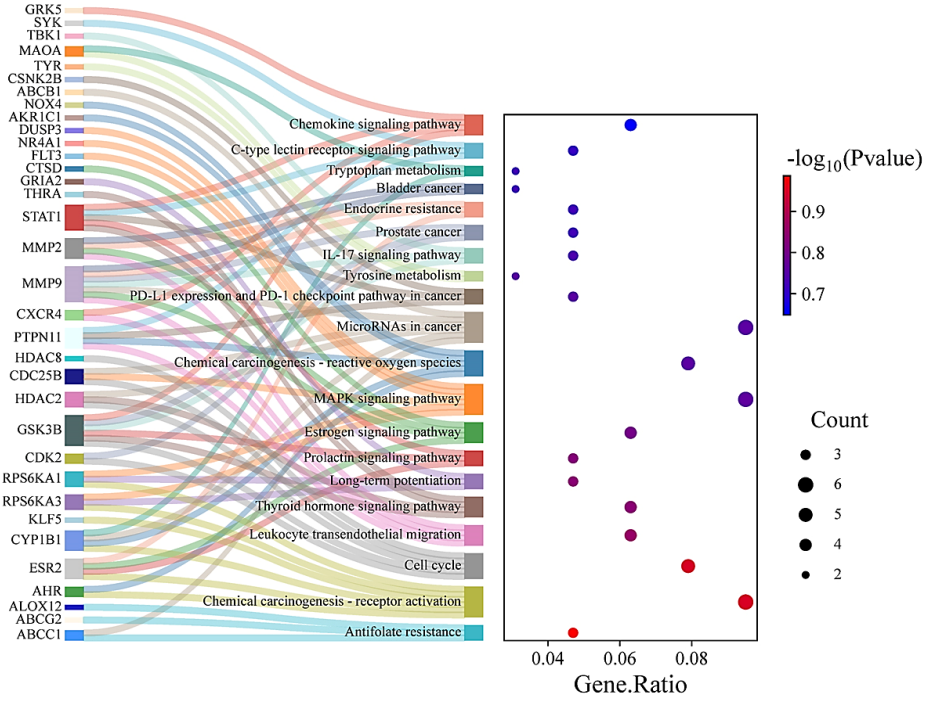

Figure S5: KEGG pathway enrichment analysis shown by Sankey dot plot, illustrating significant signaling and metabolic pathways modulated by kaempferol's hub targets, including MAPK signaling, PD-1/PD-L1 checkpoint regulation, and cancer-specific pathways.

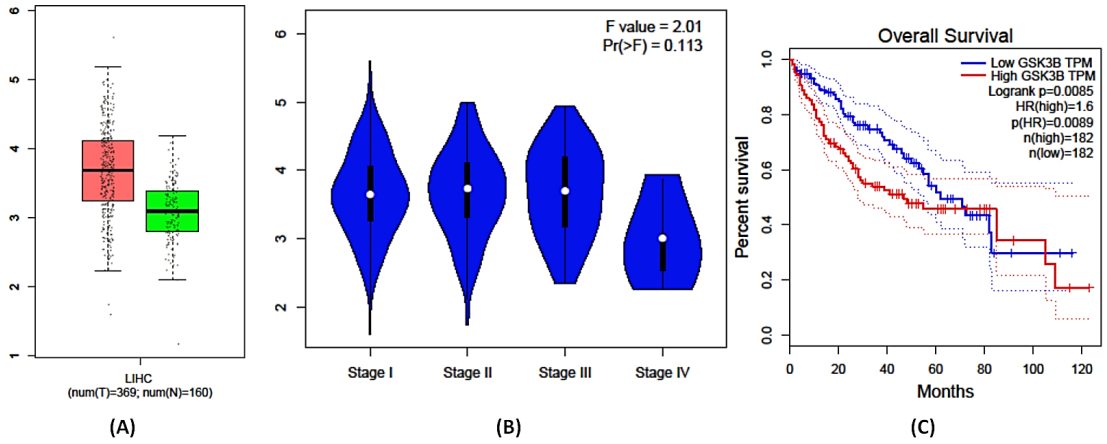

Figure S6: (A) GSK3B expression levels in liver cancer tumor tissues versus normal tissues, showing a marked increase in tumors, highlighting its oncogenic role. (B) Stage-specific expression of GSK3B in liver cancer, showing stable expression across stages I-III and a significant reduction at stage IV. (C) Kaplan-Meier survival analysis showing an inverse correlation between GSK3B expression and patient survival, with lower GSK3B expression linked to better outcomes.

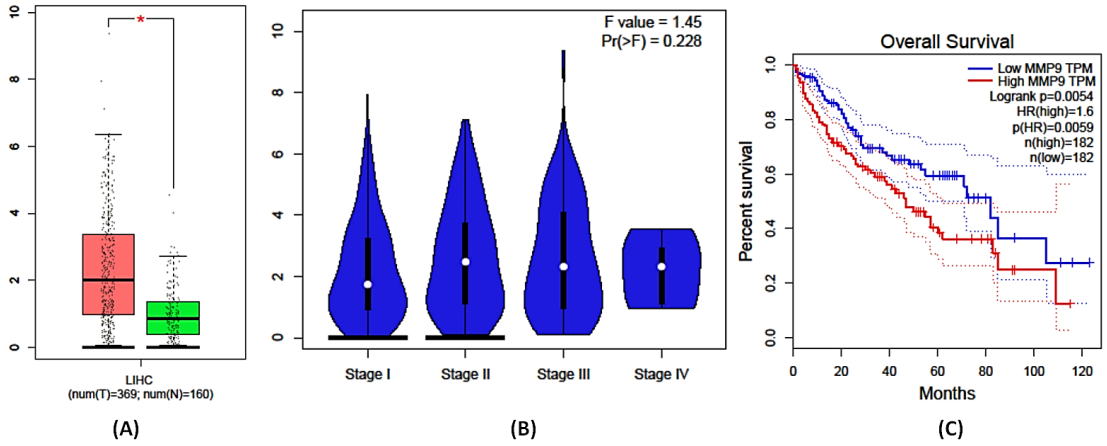

Figure S7: (A) MMP9 expression comparison between liver tumor tissues and normal tissues, revealing significantly elevated expression in tumors, indicative of its role in tumor progression. (B) Stage-specific analysis of MMP9 expression, showing progressive increases from stage I to IV, correlating with advancing disease severity. (C) Kaplan-Meier survival analysis showing improved survival rates associated with lower MMP9 expression, highlighting its prognostic significance.

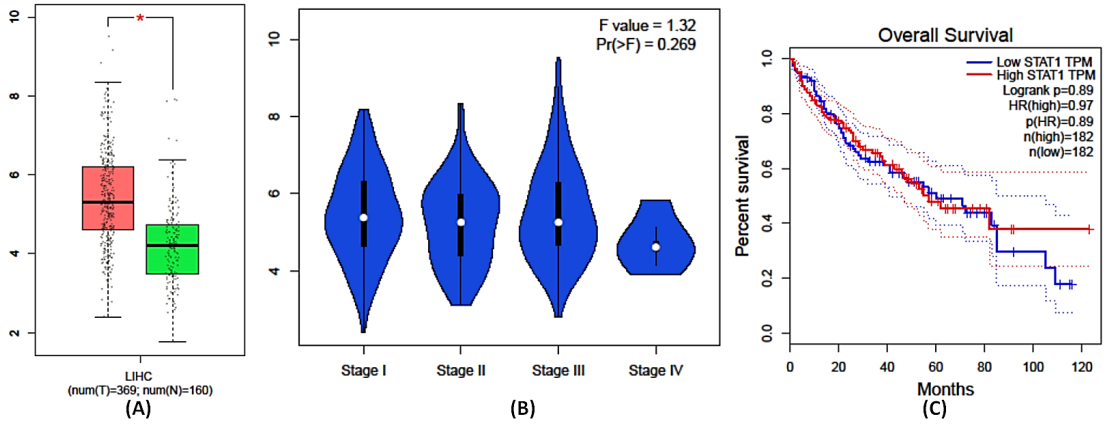

Figure S8: (A) STAT1 expression levels in liver cancer tumor tissues compared to normal tissues, with a notable increase in tumor tissues, suggesting its involvement in cancer biology. (B) Stage-specific analysis of STAT1 expression, showing a gradual decline from stage I to IV, possibly reflecting changes in tumor biology. (C) Kaplan-Meier survival analysis showing a complex relationship between STAT1 expression and patient outcomes, with both high and low expression linked to variable survival rates.

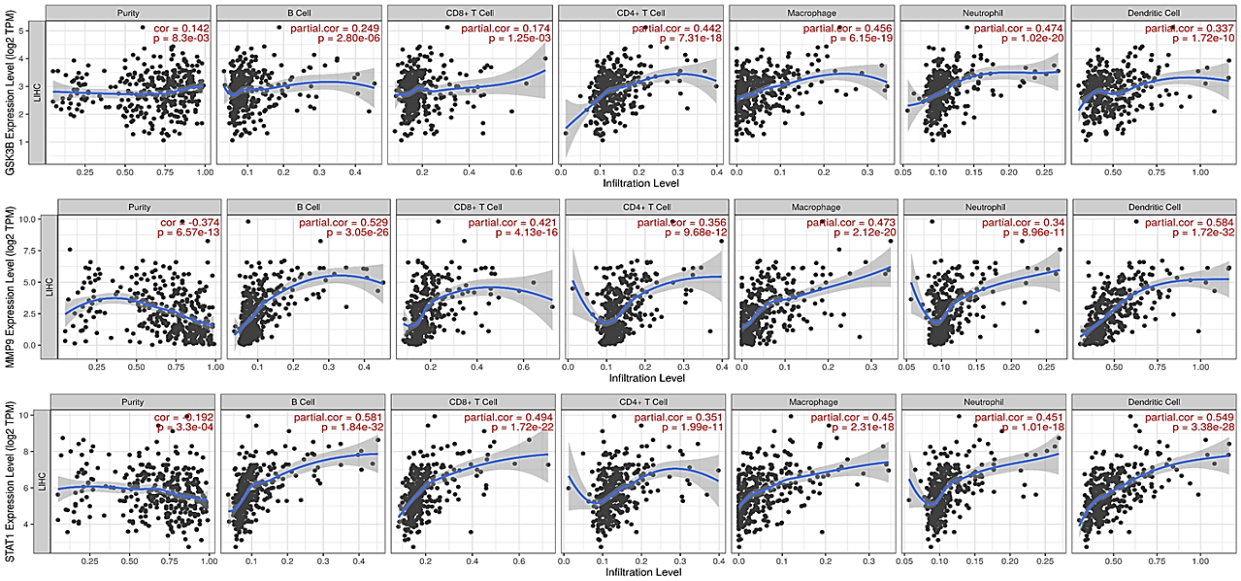

Figure S9: Correlation between the expression of GSK3B, MMP9, and STAT1 and immune cell infiltration in liver cancer, as determined by TIMER analysis, highlighting their differential associations with immune cells like macrophages, T cells, and dendritic cells.

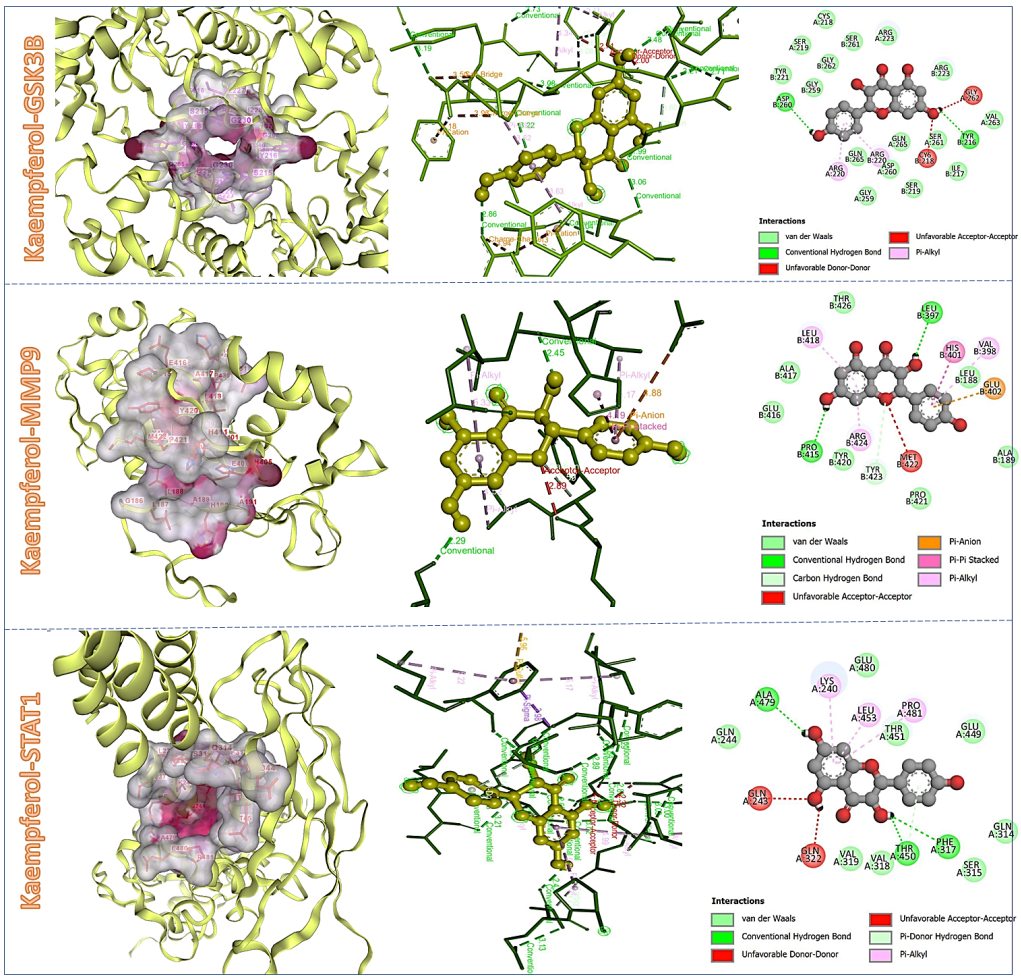

Figure S10: Docking interactions of kaempferol with GSK3B, MMP9, and STAT1. The figure shows 3D and 2D representations of kaempferol binding to GSK3B, MMP9, and STAT1. Kaempferol displayed the strongest affinity for MMP9 (-9.2 kcal/mol), followed by GSK3B (-8.9 kcal/mol) and STAT1 (-7.0 kcal/mol). Binding site cavity volumes were 889 Å^3 (GSK3B), 585 Å^3 (MMP9), and 709 Å^3 (STAT1). Interactions included hydrogen bonds, hydrophobic contacts, and π-π stacking with key residues, demonstrating multi-interactions of Kaempferol with the liver cancer related hub genes.

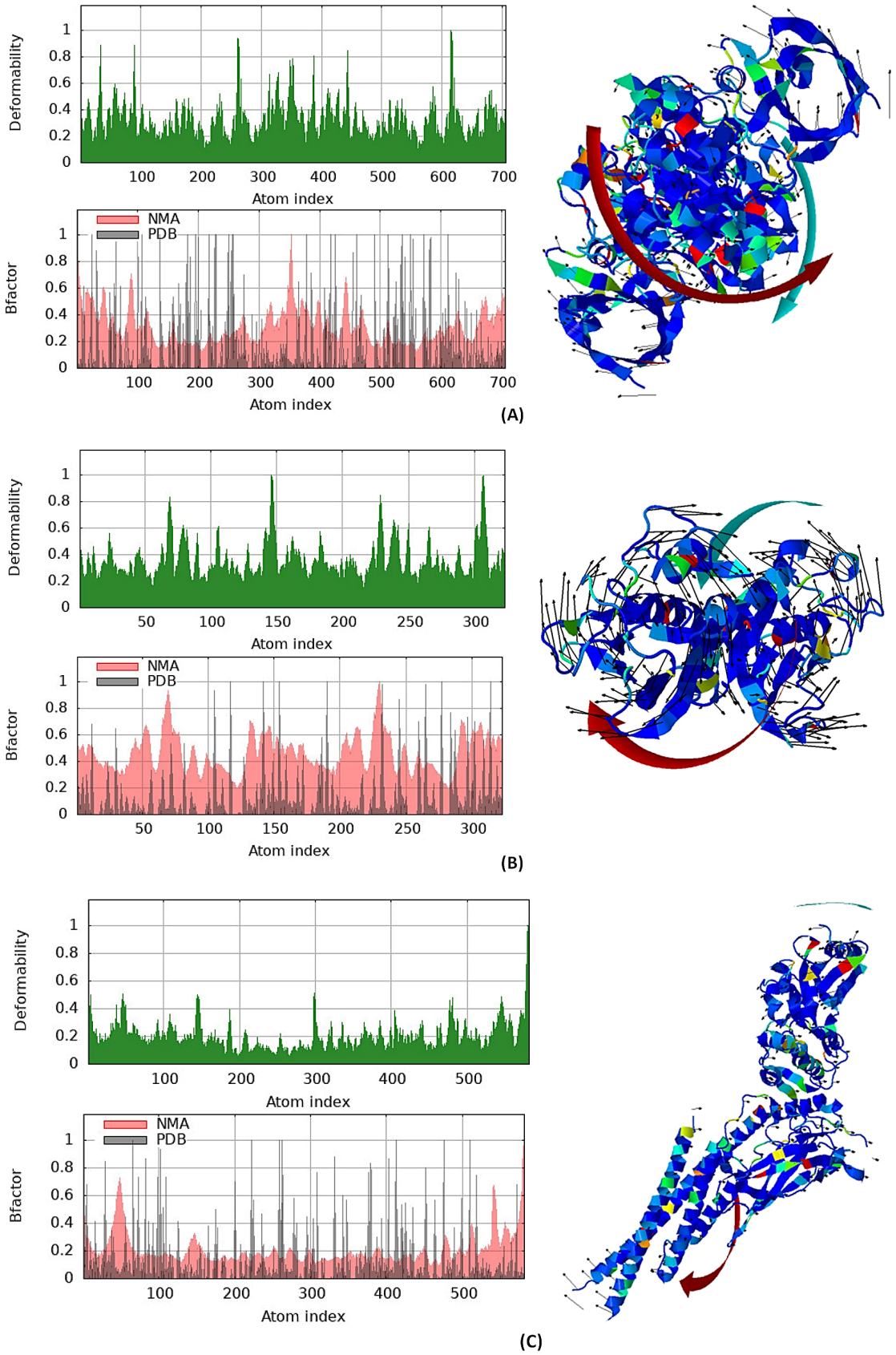

Figure S11: Deformability and beta factor (B-factor) analysis of the docked complexes, showing flexible and rigid regions within (A) GSK3B, (B) MMP9, and (C) STAT1. Higher flexibility near the ligand-binding sites indicates structural adaptability, while the rigid core regions contribute to protein stability.